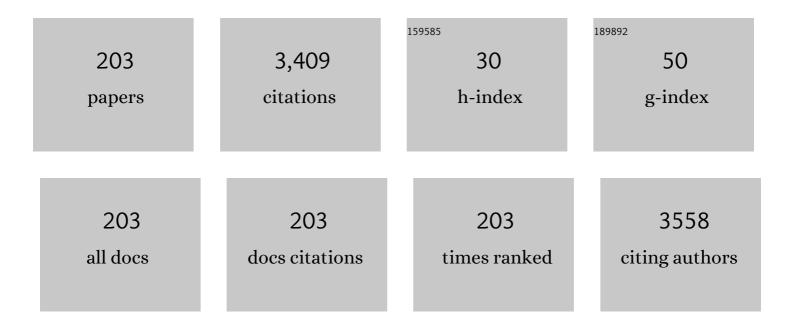
Minkyu Je

List of Publications by Year in descending order

Source: https://exaly.com/author-pdf/9374245/publications.pdf Version: 2024-02-01



MINKVILLE

#	Article	IF	CITATIONS
1	A 46-nF/10-MΩ Range 114-aF/0.37-Ω Resolution Parasitic- and Temperature-Insensitive Reconfigurable RC-to-Digital Converter in 0.18- <i>μ</i> m CMOS. IEEE Transactions on Circuits and Systems I: Regular Papers, 2022, 69, 1171-1184.	5.4	2
2	A Multimodal Neural-Recording IC With Reconfigurable Analog Front-Ends for Improved Availability and Usability for Recording Channels. IEEE Transactions on Biomedical Circuits and Systems, 2022, 16, 185-199.	4.0	8
3	An Impedance Readout IC with Ratio-Based Measurement Techniques for Electrical Impedance Spectroscopy. Sensors, 2022, 22, 1563.	3.8	9
4	On-Chip Sinusoidal Signal Generators for Electrical Impedance Spectroscopy: Methodological Review. IEEE Transactions on Biomedical Circuits and Systems, 2022, 16, 337-360.	4.0	10
5	An SRAM-Based Hybrid Computation-in-Memory Macro Using Current-Reused Differential CCO. IEEE Journal on Emerging and Selected Topics in Circuits and Systems, 2022, 12, 536-546.	3.6	4
6	Dynamic-Range-Enhancement Techniques for Artifact-Tolerant Biopotential-Acquisition ICs. IEEE Transactions on Circuits and Systems II: Express Briefs, 2022, 69, 3090-3095.	3.0	1
7	Advances in Wearable Brain-Computer Interfaces From an Algorithm-Hardware Co-Design Perspective. IEEE Transactions on Circuits and Systems II: Express Briefs, 2022, 69, 3071-3077.	3.0	3
8	A Reconfigurable Neural Stimulation IC With a High-Resolution Strength Control and <i>In-Situ</i> Neural Recording Function for Cochlear Implant Systems. IEEE Solid-State Circuits Letters, 2022, 5, 162-165.	2.0	4
9	A Wide-Dynamic-Range Neural-Recording IC With Automatic-Gain-Controlled AFE and CT Dynamic-Zoom ΔΣ ADC for Saturation-Free Closed-Loop Neural Interfaces. IEEE Journal of Solid-State Circuits, 2022, 57, 3071-3082.	5.4	6
10	Energy-Efficient High-Voltage Pulsers for Ultrasound Transducers. IEEE Transactions on Circuits and Systems II: Express Briefs, 2021, 68, 19-23.	3.0	11
11	A Precise Lesion Localization System Using a Magnetometer With Real-Time Baseline Cancellation for Laparoscopic Surgery. IEEE Access, 2021, 9, 131648-131657.	4.2	0
12	Multimodal Neural Interface Circuits for Diverse Interaction With Neuronal Cell Population in Human Brain. IEEE Transactions on Circuits and Systems II: Express Briefs, 2021, 68, 574-580.	3.0	4
13	Logic Device Based on Skyrmion Annihilation. IEEE Transactions on Electron Devices, 2021, 68, 1939-1943.	3.0	20
14	A 5.7µW/Channel Folded-Current-Mirror-Based Reconfigurable Multimodal Neural Recording IC with Improved Hardware Availability. , 2021, , .		1
15	A 67-pJ/Bit 435-MHz 16-QAM Modulator for Capsule Endoscopy System with 18-ns Start-Up Using Transient DC Error Correction. , 2021, , .		0
16	A Power-Efficient, Wide-Frequency-Range Impedance Measurement IC Using Frequency-Shift Technique. , 2021, , .		2
17	Subthreshold electrical stimulation as a low power electrical treatment for stroke rehabilitation. Scientific Reports, 2021, 11, 14048.	3.3	4
18	A Neural Recording and Stimulation Chip with Artifact Suppression for Biomedical Devices. Journal of Healthcare Engineering, 2021, 2021, 1-11.	1.9	2

#	Article	IF	CITATIONS
19	A High-Precision Single-Ended-Current-to-Differential-Voltage Converter for Reconfigurable Neural Recording Front-Ends. , 2021, , .		1
20	A Multimodal Neural Activity Readout Integrated Circuit for Recording Fluorescence and Electrical Signals. IEEE Access, 2021, 9, 118610-118623.	4.2	3
21	A Load-Current-Regulating OLED Lamp Driver Using a Hybrid Step-Up Converter with 93.21% Efficiency at a High Conversion Ratio of 4.1. , 2021, , .		0
22	A Wireless Power and Data Transfer IC for Neural Prostheses Using a Single Inductive Link With Frequency-Splitting Characteristic. IEEE Transactions on Biomedical Circuits and Systems, 2021, 15, 1306-1319.	4.0	13
23	A Polar-Demodulation-Based Impedance-Measurement IC Using Frequency-Shift Technique With Low Power Consumption and Wide Frequency Range. IEEE Transactions on Biomedical Circuits and Systems, 2021, 15, 1210-1220.	4.0	7
24	A Neural Stimulation IC Based on a Reconfigurable Current DAC with In-Situ Neural Recording Function for Cochlear Implant Systems. , 2021, , .		2
25	Radiation-Hardened Sensor Interface Circuit for Monitoring Severe Accidents in Nuclear Power Plants. IEEE Transactions on Nuclear Science, 2020, 67, 1738-1745.	2.0	13
26	A CMRR Enhancement Circuit Employing Gâ,~-Controllable Output Stages for Capacitively Coupled Instrumentation Amplifiers. IEEE Transactions on Circuits and Systems II: Express Briefs, 2020, 67, 1539-1543.	3.0	4
27	A 1.0 V, 5.4 pJ/bit GFSK Demodulator Based on an Injection Locked Ring Oscillator for Low-IF Receivers. IEEE Access, 2020, 8, 185209-185217.	4.2	1
28	Implantable Neural-Recording Modules for Monitoring Electrical Neural Activity in the Central and Peripheral Nervous Systems. , 2020, , .		3
29	An Energy-Efficient Three-Stage Amplifier Achieving a High Unity-Gain Bandwidth for Large Capacitive Loads Without Using a Compensation Zero. IEEE Solid-State Circuits Letters, 2020, 3, 530-533.	2.0	3
30	A Multi-Mode ULP Receiver Based on an Injection-Locked Oscillator for IoT Applications. IEEE Access, 2020, 8, 76966-76979.	4.2	5
31	Double-High-Pass-Filter-Based Electrical-Recording Front-Ends and Fluorescence-Recording Front-Ends for Monitoring Multimodal Neural Activity. IEEE Transactions on Circuits and Systems II: Express Briefs, 2020, 67, 876-880.	3.0	7
32	A Power-Efficient Radiation Sensor Interface with a Peak-Triggered Sampling Scheme for Mobile Dosimeters. Sensors, 2020, 20, 3255.	3.8	5
33	An Ultra-Low-Noise Swing-Boosted Differential Relaxation Oscillator in 0.18- <i>μ</i> m CMOS. IEEE Journal of Solid-State Circuits, 2020, 55, 2489-2497.	5.4	29
34	Design of Reconfigurable Time-to-Digital Converter Based on Cascaded Time Interpolators for Electrical Impedance Spectroscopy. Sensors, 2020, 20, 1889.	3.8	8
35	Input-Adaptive and Regulated Multi-Output Power Management Unit for Wireless Power Reception and Distribution in Multi-Unit Implantable Devices. , 2020, , .		3
36	A High DR, DC-Coupled, Time-Based Neural-Recording IC With Degeneration R-DAC for Bidirectional Neural Interface. IEEE Journal of Solid-State Circuits, 2019, 54, 2658-2670.	5.4	38

#	Article	IF	CITATIONS
37	Smartphone-based multispectral imaging and machine-learning based analysis for discrimination between seborrheic dermatitis and psoriasis on the scalp. Biomedical Optics Express, 2019, 10, 879.	2.9	24
38	Plugging Electronics Into Minds: Recent Trends and Advances in Neural Interface Microsystems. IEEE Solid-State Circuits Magazine, 2019, 11, 29-42.	0.4	8
39	An Area-Efficient Rectifier with Threshold Voltage Cancellation for Intra-Body Power Transfer. , 2019, , .		11
40	Introduction to the Special Issue on the 2019 IEEE Symposium on VLSI Circuits. IEEE Solid-State Circuits Letters, 2019, 2, 272-272.	2.0	0
41	A Reconfigurable Neural Recording Front-End IC for Multimodal Operation. , 2019, , .		2
42	A Level Shifter for CMRR-Enhanced Biopotential Acquisition Systems with Human-Body-Coupled Floating Supply Domain. , 2019, , .		0
43	A Sub-\${mu}\$W/Ch Analog Front-End for \$Delta \$-Neural Recording With Spike-Driven Data Compression. IEEE Transactions on Biomedical Circuits and Systems, 2019, 13, 1-14.	4.0	36
44	A 1-V 4.6-μW/channel Fully Differential Neural Recording Front-end IC with Current-controlled Pseudoresistor in 0.18-μm CMOS. Journal of Semiconductor Technology and Science, 2019, 19, 30-41.	0.4	2
45	An ultra-low-noise differential relaxation oscillator based on a swing-boosting scheme. , 2018, , .		0
46	Design of an On-Silicon-Interposer Passive Equalizer for Next Generation High Bandwidth Memory With Data Rate Up To 8 Gb/s. IEEE Transactions on Circuits and Systems I: Regular Papers, 2018, 65, 2293-2303.	5.4	16
47	A powerâ€efficient currentâ€mode neural/muscular stimulator design for peripheral nerve prosthesis. International Journal of Circuit Theory and Applications, 2018, 46, 692-706.	2.0	11
48	A 4.86 µW/Channel Fully Differential Multi-Channel Neural Recording System. , 2018, , .		0
49	Technical Review: Interface Integrated Circuits for Metal-Oxide GAS Sensors. , 2018, , .		1
50	Technical Review: Electromagnetic Sensor System for Localization of Medical Devices. , 2018, , .		1
51	A 650-uW 30-Mbps Galvanic Coupling Communication Receiver for Bionic Arms. , 2018, , .		0
52	A Sinusoidal Signal Generator Using a Constant Gain Finite Impulse Response (FIR) Filter for Electrical Bioimpedance Spectroscopy. , 2018, , .		8
53	Analysis of acetabular orientation and femoral anteversion using images of three-dimensional reconstructed bone models. International Journal of Computer Assisted Radiology and Surgery, 2017, 12, 855-864.	2.8	6
54	Multispectral imaging based on a Smartphone with an external C-MOS camera for detection of seborrheic dermatitis on the scalp. Proceedings of SPIE, 2017, , .	0.8	0

#	Article	IF	CITATIONS
55	Enhancement of Interface Characteristics of Neural Probe Based on Graphene, ZnO Nanowires, and Conducting Polymer PEDOT. ACS Applied Materials & Interfaces, 2017, 9, 10577-10586.	8.0	47
56	A Resonator-Adaptable Oscillator Using Varactor-Loaded Tuned Amplifiers. IEEE Microwave and Wireless Components Letters, 2017, 27, 724-726.	3.2	6
57	Smart Sensor Microsystems: Application-Dependent Design and Integration Approaches. , 2017, , 83-107.		1
58	An artifact-suppressed stimulator for simultaneous neural recording and stimulation systems. , 2017, 2017, 2017, 2118-2121.		4
59	A neural recording amplifier based on adaptive SNR optimization technique for long-term implantation. , 2017, , .		2
60	A simultaneous neural recording and stimulation system using signal folding in recording circuits. , 2017, , .		0
61	A novel smart navigation system for intramedullary nailing in orthopedic surgery. PLoS ONE, 2017, 12, e0174407.	2.5	12
62	Independent Mobility Achieved through a Wireless Brain-Machine Interface. PLoS ONE, 2016, 11, e0165773.	2.5	30
63	Smartphone-based multispectral imaging: system development and potential for mobile skin diagnosis. Biomedical Optics Express, 2016, 7, 5294.	2.9	65
64	Parasitic analysis and π-type Butterworth-Van Dyke model for complementary-metal-oxide-semiconductor Lamb wave resonator with accurate two-port Y-parameter characterizations. Review of Scientific Instruments, 2016, 87, 045004.	1.3	18
65	A 0.8 V Supply- and Temperature-Insensitive Capacitance-to-Digital Converter in 0.18- <inline-formula> <tex-math notation="LaTeX">\$mu ext{m}\$ </tex-math> </inline-formula> CMOS. IEEE Sensors Journal, 2016, 16, 5354-5364.	4.7	16
66	Design considerations and approaches for sensor interface circuits in smart sensor microsystems. , 2016, , .		0
67	Low-energy integrated circuits and microsystems for implantable wireless neural recording. , 2016, , .		0
68	An Integrated Wireless Power Management and Data Telemetry IC for High-Compliance-Voltage Electrical Stimulation Applications. IEEE Transactions on Biomedical Circuits and Systems, 2016, 10, 113-124.	4.0	27
69	A Low Switching-Loss W-Band Radiometer Utilizing a Single-Pole-Double-Throw Distributed Amplifier in 0.13- <formula formulatype="inline"> <tex notation="TeX">\$mu{hbox {m}}\$</tex> </formula> SiGe BiCMOS. IEEE Transactions on Microwave Theory and Techniques, 2016, 64, 226-238.	4.6	27
70	A 9â€bit successive approximation ADC in SOI CMOS operating up to 300 °C. International Journal of Circuit Theory and Applications, 2016, 44, 418-427.	2.0	3
71	An implantable neural recording IC with In-Situ spike detection and preservation. , 2015, , .		0
72	A \$1.5pm 0.39~{m ppm}/^{circ}{m C}\$ Temperature-Compensated LC Oscillator Using Constant-Biased Varactors. IEEE Microwave and Wireless Components Letters, 2015, 25, 130-132.	3.2	8

#	Article	IF	CITATIONS
73	A pulse-width-adaptive active charge balancing circuit with pulse-insertion based residual charge compensation and quantization for electrical stimulation applications. , 2015, , .		7
74	Wireless sensor microsystems for emerging biomedical applications (Invited). , 2015, , .		2
75	An Ultralow-Voltage Sensor Node Processor With Diverse Hardware Acceleration and Cognitive Sampling for Intelligent Sensing. IEEE Transactions on Circuits and Systems II: Express Briefs, 2015, 62, 1149-1153.	3.0	10
76	A Fully Integrated Temperature-Independent Reconfigurable Acoustic Transmitter With Digital On-Chip Resistor Temperature Coefficient Calibration for Oil Drilling Application. IEEE Transactions on Circuits and Systems II: Express Briefs, 2015, 62, 553-557.	3.0	1
77	An Ultra-Low Voltage Level Shifter Using Revised Wilson Current Mirror for Fast and Energy-Efficient Wide-Range Voltage Conversion from Sub-Threshold to I/O Voltage. IEEE Transactions on Circuits and Systems I: Regular Papers, 2015, 62, 697-706.	5.4	70
78	Design of an Ultra-low Voltage 9T SRAM With Equalized Bitline Leakage and CAM-Assisted Energy Efficiency Improvement. IEEE Transactions on Circuits and Systems I: Regular Papers, 2015, 62, 441-448.	5.4	66
79	An Energy Autonomous 400 MHz Active Wireless SAW Temperature Sensor Powered by Vibration Energy Harvesting. IEEE Transactions on Circuits and Systems I: Regular Papers, 2015, 62, 976-985.	5.4	24
80	A 16-channel 24-V 1.8-mA power efficiency enhanced neural/muscular stimulator with exponentially decaying stimulation current. , 2015, , .		8
81	Fast and energy-efficient low-voltage level shifters. Microelectronics Journal, 2015, 46, 75-80.	2.0	9
82	BIST Methodology, Architecture and Circuits for Pre-Bond TSV Testing in 3D Stacking IC Systems. IEEE Transactions on Circuits and Systems I: Regular Papers, 2015, 62, 139-148.	5.4	30
83	Near-Threshold Energy- and Area-Efficient Reconfigurable DWPT/DWT Processor for Healthcare-Monitoring Applications. IEEE Transactions on Circuits and Systems II: Express Briefs, 2015, 62, 70-74.	3.0	29
84	A sub-threshold to super-threshold Level Conversion Flip Flop for sub/near-threshold dual-supply operation. , 2014, , .		1
85	A 20V-compliance implantable neural stimulator IC with closed-loop power control, active charge balancing, and electrode impedance check. , 2014, , .		12
86	A 0.5-V sub-μW/channel neural recording IC with delta-modulation-based spike detection. , 2014, , .		7
87	A 103 pJ/bit multi-channel reconfigurable GMSK/PSK/16-QAM transmitter with band-shaping. , 2014, , .		6
88	A Digitally Assisted, Signal Folding Neural Recording Amplifier. IEEE Transactions on Biomedical Circuits and Systems, 2014, 8, 528-542.	4.0	35
89	A high-sensitivity 135GHz millimeter-wave imager by differential transmission-line loaded split-ring-resonator in 65nm CMOS. , 2014, , .		1
90	A Low Power Interference Robust IR-UWB Transceiver SoC for WBAN Applications. , 2014, , 23-44.		3

A Low Power Interference Robust IR-UWB Transceiver SoC for WBAN Applications. , 2014, , 23-44. 90

#	Article	IF	CITATIONS
91	A single-input dual-output 13.56MHz CMOS AC–DC converter with comparator-driven rectifiers for implantable devices. Microelectronics Journal, 2014, 45, 277-281.	2.0	14
92	30.7 A 60Mb/s wideband BCC transceiver with 150pJ/b RX and 31pJ/b TX for emerging wearable applications. , 2014, , .		21
93	A Fixed-frequency hysteretic controlled buck DC-DC converter with improved load regulation. , 2014, ,		8
94	Fast Location of Opens in TSV-Based 3-D Chip Using Simple Resistor Chain. IEEE Transactions on Electron Devices, 2014, 61, 2584-2587.	3.0	1
95	Design and in Vitro Test of a Differentially Fed Dual-Band Implantable Antenna Operating at MICS and ISM Bands. IEEE Transactions on Antennas and Propagation, 2014, 62, 2430-2439.	5.1	128
96	A Reference-Less Injection-Locked Clock-Recovery Scheme for Multilevel-Signaling-Based Wideband BCC Receivers. IEEE Transactions on Microwave Theory and Techniques, 2014, 62, 1856-1866.	4.6	9
97	High Bandwidth Efficiency and Low Power Consumption Walsh Code Implementation Methods for Body Channel Communication. IEEE Transactions on Microwave Theory and Techniques, 2014, 62, 1867-1878.	4.6	33
98	A Monolithically Integrated Pressure/Oxygen/Temperature Sensing SoC for Multimodality Intracranial Neuromonitoring. IEEE Journal of Solid-State Circuits, 2014, 49, 2449-2461.	5.4	31
99	A 457 nW Near-Threshold Cognitive Multi-Functional ECG Processor for Long-Term Cardiac Monitoring. IEEE Journal of Solid-State Circuits, 2014, 49, 2422-2434.	5.4	28
100	Temperature Sensor Front End in SOI CMOS Operating up to 250 <inline-formula> <tex-math notation="TeX">\$^{circ}hbox{C}\$</tex-math </inline-formula> . IEEE Transactions on Circuits and Systems II: Express Briefs, 2014, 61, 496-500.	3.0	6
101	A 0.5V 29pJ/cycle sensor node processor for intelligent sensing applications. , 2014, , .		1
102	Analysis and Design of Gain Enhanced Cascode Stage Utilizing a New Passive Compensation Network. IEEE Transactions on Microwave Theory and Techniques, 2013, 61, 2892-2900.	4.6	6
103	A CMOS High-Voltage Transmitter IC for Ultrasound Medical Imaging Applications. IEEE Transactions on Circuits and Systems II: Express Briefs, 2013, 60, 316-320.	3.0	35
104	A flexible polyimide cable for implantable neural probe arrays. Microsystem Technologies, 2013, 19, 1111-1118.	2.0	11
105	A wireless power management and data telemetry circuit module for high compliance voltage electrical stimulation applications. , 2013, , .		9
106	A 0.45 V 100-Channel Neural-Recording IC With Sub- <formula formulatype="inline"><tex Notation="TeX">\$mu {m W}\$</tex </formula> /Channel Consumption in 0.18 <formula formulatype="inline"><tex notation="TeX">\$mu{m m}\$</tex></formula> CMOS. IEEE Transactions on Biomedical Circuits and Systems, 2013, 7,	4.0	115
107	735-746. A low-profile three-dimensional neural probe array using a silicon lead transfer structure. Journal of Micromechanics and Microengineering, 2013, 23, 095013.	2.6	13

108 Energy efficient transmitters for high data rate biomedical applications. , 2013, , .

0

#	Article	IF	CITATIONS
109	A 0.5V 16nW 8.08-ENOB SAR ADC for ultra-low power sensor applications. , 2013, , .		5
110	RFDAC for medical body area network applications. , 2013, , .		0
111	HEPP: A new in-situ timing-error prediction and prevention technique for variation-tolerant ultra-low-voltage designs. , 2013, , .		30
112	Design of high-efficiency inductive power transfer coils for biomedical implants. , 2013, , .		3
113	Electric near-field coupling for wireless power transfer in biomedical applications. , 2013, , .		28
114	A fast and energy-efficient level shifter with wide shifting range from sub-threshold up to I/O voltage. , 2013, , .		19
115	A time-domain smart temperature sensor without an explicit bandgap reference in SOI CMOS operating up to 225°C. , 2013, , .		3
116	An energy-autonomous piezoelectric energy harvester interface circuit with 0.3V startup voltage. , 2013, , .		6
117	A pressure/oxygen/temperature sensing SoC for multimodality intracranial neuromonitoring. , 2013, , .		3
118	A 457-nW cognitive multi-functional ECG processor. , 2013, , .		8
119	Data rate enhancement method for body channel frequency selective digital transmission scheme. , 2013, , .		2
120	A Crystal-Less Temperature-Independent Reconfigurable Transmitter Targeted for High-Temperature Wireless Acoustic Telemetry Applications. IEEE Transactions on Circuits and Systems II: Express Briefs, 2013, 60, 542-546.	3.0	2
121	CMUT ultrasonic power link front-end for wireless power transfer deep in body. , 2013, , .		5
122	Implantable stimulator for biomedical applications. , 2013, , .		0
123	Digital system design for wireless bionic neural link. , 2013, , .		0
124	A high-frequency transimpedance amplifier for CMOS integrated 2D CMUT array towards 3D ultrasound imaging. , 2013, 2013, 101-4.		7
125	A Current-Switching and \$g _{m}\$-Enhanced Colpitts Quadrature VCO. IEEE Microwave and Wireless Components Letters, 2013, 23, 143-145.	3.2	22
126	A 19.2 mW, \${> 45}~{m dB}\$ Gain and High-Selectivity 94 GHz LNA in 0.13 \$mu{m m}\$ SiGe BiCMOS. IEEE Microwave and Wireless Components Letters, 2013, 23, 261-263.	3.2	17

#	Article	IF	CITATIONS
127	High-Efficiency Wireless Power Transfer for Biomedical Implants by Optimal Resonant Load Transformation. IEEE Transactions on Circuits and Systems I: Regular Papers, 2013, 60, 867-874.	5.4	270
128	A 100-Channel 1-mW Implantable Neural Recording IC. IEEE Transactions on Circuits and Systems I: Regular Papers, 2013, 60, 2584-2596.	5.4	104
129	A Thermal Isolation Technique Using Through-Silicon Vias for Three-Dimensional ICs. IEEE Transactions on Electron Devices, 2013, 60, 1282-1287.	3.0	11
130	A 100 Mb/s 0.36 mW injection locked clock and data recovery circuit for WBAN transceivers. , 2013, , .		2
131	Future mobile society beyond Moore's Law. , 2013, , .		1
132	25 to 300 Degree celsius 80bps acoustic transmitter based on crystal-less temperature-independent frequency reference with differential modulation for drilling noise power cancellation. , 2013, , .		0
133	An Asymmetrical QPSK/OOK Transceiver SoC and 15:1 JPEG Encoder IC for Multifunction Wireless Capsule Endoscopy. IEEE Journal of Solid-State Circuits, 2013, 48, 2717-2733.	5.4	19
134	Automated Measures of Hand Hygiene Compliance among Healthcare Workers Using Ultrasound: Validation and a Randomized Controlled Trial. Infection Control and Hospital Epidemiology, 2013, 34, 919-928.	1.8	54
135	A 0.18V charge-pumped DFF with 50.8% energy-delay reduction for near-/sub-threshold circuits. , 2013, ,		5
136	Neural recording front-end IC using action potential detection and analog buffer with digital delay for data compression. , 2013, 2013, 747-50.		16
137	Development of flexible neural probes using SU-8/parylene. , 2013, , .		2
138	A 110pJ/b multichannel FSK/GMSK/QPSK/p/4-DQPSK transmitter with phase-interpolated dual-injection DLL-based synthesizer employing hybrid FIR. , 2013, , .		10
139	A low power, 900MHz fractional-N synthesizer with quadrature outputs in 0.13um CMOS. , 2013, , .		0
140	Passives design for a high performance W-band amplifier. , 2013, , .		2
141	Cytocompatibility Assessment of Si, Plasma Enhanced Chemical Vapor Deposition-Formed SiO2 and Si3N4 Used for Neural Prosthesis: A Comparative Study. Nanoscience and Nanotechnology Letters, 2013, 5, 916-920.	0.4	3
142	High-speed CMOS image sensor for high-throughput lensless microfluidic imaging system. Proceedings of SPIE, 2012, , .	0.8	8
143	Geometric scalable 2-port center-tap inductor modeling. , 2012, , .		3
144	Investigation of the mutual effect between power link and data link for biomedicai applications. , 2012,		0

#	Article	IF	CITATIONS
145	A hardware-efficient all-digital transmitter architecture for acoustic borehole telemetry systems. , 2012, , .		2
146	A low power interference robust IR-UWB transceiver SoC for WBAN applications. , 2012, , .		7
147	Ultra-low-energy near-threshold biomedical signal processor for versatile wireless health monitoring. , 2012, , .		7
148	100-Channel wireless neural recording system with 54-Mb/s data link and 40%-efficiency power link. , 2012, , .		18
149	An efficient wireless power link for neural implant. , 2012, , .		3
150	A digitally assisted, pseudo-resistor-less amplifier in 65nm CMOS for neural recording applications. , 2012, , .		3
151	800â€nW 43â€nV/[radical]Hz neural recording amplifier with enhanced noise efficiency factor. Electronics Letters, 2012, 48, 479.	1.0	47
152	A 60-V, \$>hbox{225} ^{circ}hbox{C}\$ Half-Bridge Driver for Piezoelectric Acoustic Transducer, on SOI CMOS. IEEE Transactions on Circuits and Systems II: Express Briefs, 2012, 59, 771-775.	3.0	2
153	A 1.8V 1MS/s rail-to-rail 10-bit SAR ADC in 0.18μm CMOS. , 2012, , .		9
154	A signal folding neural amplifier exploiting neural signal statistics. , 2012, , .		1
155	A 0.2V 16Kb 9T SRAM with bitline leakage equalization and CAM-assisted write performance boosting for improving energy efficiency. , 2012, , .		5
156	Self-test methodology and structures for pre-bond TSV testing in 3D-IC system. , 2012, , .		5
157	An inductively powered CMOS multichannel bionic neural link for peripheral nerve function restoration. , 2012, , .		8
158	A wirelessly powered and interrogated blood flow monitoring microsystem fully integrated with a prosthetic vascular graft for early failure detection. , 2012, , .		6
159	An asymmetrical QPSK/OOK transceiver SoC and 15:1 JPEG encoder IC for multifunction wireless capsule endoscopy. , 2012, , .		3
160	Computing mutual inductance between spatially misaligned coils for wireless power transmission. , 2012, , .		3
161	Low power implantable neural recording front-end. , 2012, , .		2
162	A Self-Powered Power Conditioning IC for Piezoelectric Energy Harvesting From Short-Duration Vibrations. IEEE Transactions on Circuits and Systems II: Express Briefs, 2012, 59, 578-582.	3.0	30

#	Article	IF	CITATIONS
163	A Low-Power Variable-Gain Amplifier With Improved Linearity: Analysis and Design. IEEE Transactions on Circuits and Systems I: Regular Papers, 2012, 59, 2176-2185.	5.4	37
164	A CMOS Rectifier With a Cross-Coupled Latched Comparator for Wireless Power Transfer in Biomedical Applications. IEEE Transactions on Circuits and Systems II: Express Briefs, 2012, 59, 409-413.	3.0	109
165	A 1â€V 1.2â€mW CMOS medradio receiver for biomedical applications. Microwave and Optical Technology Letters, 2012, 54, 2821-2825.	1.4	2
166	A SiGe BiCMOS Transmitter/Receiver Chipset With On-Chip SIW Antennas for Terahertz Applications. IEEE Journal of Solid-State Circuits, 2012, 47, 2654-2664.	5.4	84
167	An Inductively Powered Implantable Blood Flow Sensor Microsystem for Vascular Grafts. IEEE Transactions on Biomedical Engineering, 2012, 59, 2466-2475.	4.2	52
168	A 9.87 nW 1 kS/s 8.7 ENOB SAR ADC for implantable epileptic seizure detection microsystems. , 2012, , .		2
169	A low-cost 2.45-GHz wireless power link for biomedical devices. , 2012, , .		7
170	Differentially Fed Dual-Band Implantable Antenna for Biomedical Applications. IEEE Transactions on Antennas and Propagation, 2012, 60, 5587-5595.	5.1	82
171	A 160 nW 25 kS/s 9-bit SAR ADC for neural signal recording applications. , 2012, , .		10
172	Multiplexed detection of cardiac biomarkers in serum with nanowire arrays using readout ASIC. Biosensors and Bioelectronics, 2012, 35, 218-223.	10.1	52
173	Implantable Polyimide Cable for Multichannel High-Data-Rate Neural Recording Microsystems. IEEE Transactions on Biomedical Engineering, 2012, 59, 390-399.	4.2	9
174	A 50-Mb/s CMOS QPSK/O-QPSK Transmitter Employing Injection Locking for Direct Modulation. IEEE Transactions on Microwave Theory and Techniques, 2012, 60, 120-130.	4.6	44
175	Low-power wireless receivers for healthcare applications. , 2011, , .		0
176	Digital system for low power wireless neural recording system. , 2011, , .		1
177	High-voltage pulser for ultrasound medical imaging applications. , 2011, , .		22
178	A 3.4-mW 54.24-Mbps burst-mode injection-locked CMOS FSK transmitter. , 2011, , .		9
179	Low-Power Ultrawideband Wireless Telemetry Transceiver for Medical Sensor Applications. IEEE Transactions on Biomedical Engineering, 2011, 58, 768-772.	4.2	130
180	Multiple Functional ECG Signal is Processing for Wearable Applications of Long-Term Cardiac Monitoring. IEEE Transactions on Biomedical Engineering, 2011, 58, 380-389.	4.2	73

Μινκύα Je

#	Article	IF	CITATIONS
181	A 400-nW 19.5-fJ/Conversion-Step 8-ENOB 80-kS/s SAR ADC in 0.18- \$muhbox{m}\$ CMOS. IEEE Transactions on Circuits and Systems II: Express Briefs, 2011, 58, 407-411.	3.0	36
182	A CMOS MedRadio Receiver RF Front-End With a Complementary Current-Reuse LNA. IEEE Transactions on Microwave Theory and Techniques, 2011, 59, 1846-1854.	4.6	34
183	A miniature on-chip multi-functional ECG signal processor with 30 µW ultra-low power consumption. , 2010, 2010, 2577-80.		2
184	A 64-channel readout ASIC for nanowire biosensor array with electrical calibration scheme. , 2010, 2010, 3491-4.		3
185	Design and fabrication of Si-neuroprobe arrays. , 2010, , .		1
186	A 7.2mW 15Mbps ASK CMOS transmitter for ingestible capsule endoscopy. , 2010, , .		9
187	A 700-\$mu\$W Wireless Sensor Node SoC for Continuous Real-Time Health Monitoring. IEEE Journal of Solid-State Circuits, 2010, , .	5.4	18
188	A low-power high-performance accelerometer ASIC for high-end medical motion sensing. , 2010, 2010, 190-3.		5
189	Design of an impedance measurement system for living cell impedance spectroscopy. , 2009, , .		1
190	A precision relaxation oscillator with a self-clocked offset-cancellation scheme for implantable biomedical SoCs. , 2009, , .		73
191	A simple four-terminal small-signal model of RF MOSFETs and its parameter extraction. Microelectronics Reliability, 2003, 43, 601-609.	1.7	24
192	Gate bias dependence of the substrate signal coupling effect in RF MOSFETs. IEEE Electron Device Letters, 2003, 24, 183-185.	3.9	10
193	Accurate four-terminal RF MOSFET model accounting for the short-channel effect in the source-to-drain capacitance. , 2003, , .		5
194	A simple and accurate method for extracting substrate resistance of RF MOSFETs. IEEE Electron Device Letters, 2002, 23, 434-436.	3.9	42
195	A simple and analytical parameter-extraction method of a microwave MOSFET. IEEE Transactions on Microwave Theory and Techniques, 2002, 50, 1503-1509.	4.6	114
196	MOSFET MODELING AND PARAMETER EXTRACTION FOR RF IC'S. International Journal of High Speed Electronics and Systems, 2001, 11, 953-1006.	0.7	12
197	A silicon quantum wire transistor with one-dimensional subband effects. Solid-State Electronics, 2000, 44, 2207-2212.	1.4	39
198	Quantized Conductance Of A Gate-All-Around Silicon Quantum Wire Transistor. , 1998, , .		0

#	Article	IF	CITATIONS
199	Overestimation of oxide defects density in large test capacitors due to plasma processing. IEEE Transactions on Electron Devices, 1997, 44, 1554-1556.	3.0	3
200	A digital temperature compensated crystal oscillator using a temperature adaptive capacitor array. , 0, , .		0
201	On the large-signal CMOS modeling and parameter extraction for RF applications. , 0, , .		4
202	Extraction method for substrate resistance of RF MOSFETs. , 0, , .		0
203	A high speed and low power SOI inverter using active body-bias. , 0, , .		0